# SUPPLEMENTAL DATA

## SUPPLEMENTAL MATERIAL AND METHODS

### Culture of cell lines and primary CD8 T lymphocytes

HLA-A2$^{neg}$/TCRαβ$^{ko}$/CD8αβ$^{pos}$ Jurkat J76 T cells (defined thereafter as HLA-A2$^{neg}$ J76 CD8αβ cells) were generated following transduction of CD8α- and CD8β-encoding plasmids into the TCR α and β knock-out HLA-A2$^{neg}$ J76 T cell subline using retroviral vectors (kindly provided by Drs. I. Edes and W. Uckert; Max-Delbrück-Center, Berlin, Germany, *unpublished data*). HLA-A2$^{neg}$/J76 CD8αβ cells, HLA-A2$^{pos}$/TAP-deficient T2 cells (ATCC CRL-1992), HLA-A2$^{pos}$/NY-ESO-1$^{neg}$ NA8 cells (CVCL-S599) and HLA-A2$^{pos}$/NY-ESO-1$^{pos}$ Me275 cells (CVCL_S597) were cultured at 37°C and 5% $CO_2$ in RPMI 1640 medium supplemented with 10% fetal calf serum (FCS), 100 U/mL penicillin and 100 µg/mL streptomycin (Gibco). Primary CD8 T lymphocytes were positively enriched from peripheral blood mononuclear cells (PBMC) obtained from healthy donors using anti-CD8-coated magnetic microbeads (Miltenyi Biotec) and cultured at 37°C and 5% CO2 in RPMI supplemented with 8% human serum, 100 U/mL penicillin, 100 µg/mL streptomycin, 2 mM L-glutamine, 0.1 mg/mL kanamycin, 1 mM sodium pyruvate, 1X non-essential amino acids, 50 µM β-mercaptoethanol (Gibco) and 150 U/mL recombinant human IL-2 (gift from GlaxoSmithKline). HLA-A*0201 (A2 thereafter) status of the cells was determined by flow cytometry performed on PBMCs before CD8 isolation. A2$^{pos}$ and A2$^{neg}$ CD8 T lymphocytes were stimulated with CD3/CD28 beads (ThermoFisher) at a ratio of 1:1 for transduction and expansion, and subsequently expanded every 14-21 days by re-stimulation with 1 µM phytohemagglutinin (PHA; Oxoid) and 30 Gy-irradiated allogeneic A2$^{neg}$ PBMCs as feeders.

### Generation of CRISPR-A2 primary CD8 T cells and CRISPR-A2 NA8 tumor cells

The kinetic experiments (see Fig. 2, main manuscript) were performed on primary CD8 T cells from A2$^{pos}$ or A2$^{neg}$ healthy donors, for which donor-specific variations could be observed in the *ex vivo* expression of surface receptors (data not shown). Therefore, using the CRISPR/Cas9 technology, we generated A2$^{pos}$ (i.e. CRISPR/mock) and A2$^{neg}$ (i.e. CRISPR/A2) primary CD8 T cells sharing the same cellular background. CRISPR-A2 primary CD8 T cells and NA8 cells were produced according to the protocol by Ran et al. (1). Briefly, the 20 nucleotide-single guide (sgRNA) sequence targeting HLA-A*0201 was designed using http://CRISPR.mit.edu website and selected for high quality score (>80) to minimize off-targets. The sequence of the sgRNA is as following: GAGGGTCCGGAGTATTGGGA. An extra 5' G nucleotide was added

to the sgRNA sequence to improve U6 promoter efficiency. The oligo pairs encoding the sgRNA were annealed and ligated into a BsmBI-digested lenti-CRISPR plasmid v2 bearing Cas9 and sgRNA scaffold (Addgen plasmid #52961) to generate lenti-CRISPR-A2 plasmid. This plasmid was transfected into HEK 293T/17 cells (ATCC CRL-11268) using a standard calcium phosphate protocol for the production of lentiviral particles. The supernatant was concentrated by ultracentrifugation at 24000 g for 2h and subsequently used to infect freshly isolated $A2^{pos}$ CD8 T lymphocytes after 24h stimulation with CD3/CD28 beads ($1^{st}$ expansion) or NA8 cells to generate CRISPR-A2 ($A2^{neg}$)-CD8 T cells or CRISPR-A2 ($A2^{neg}$)-NA8 cells, respectively. Lenti-CRISPR-EGFP sgRNA 6 (Addgen plasmid #51765) was used as a mock control. Transduced cells ($A2^{neg}$) were sorted to purity with PE-labeled HLA-A2 antibody by flow cytometry (FACSAriaII, BD Biosciences).

**Generation of TCR-engineered primary CD8 T cells and J76 CD8αβ T cells**

The full-length codon-optimized TCR AV23.1 and TCR BV13.1 chain sequences of a dominant NY-ESO-$1_{157-165}$-specific T cell clone of patient LAU155 (BC1) were cloned in the pRRL lentiviral vectors, as IRES or T2A constructs. Structure-based amino acid substitutions within CDR2αβ and/or CDR3αβ loops were introduced into the wild-type (WT) TCR sequence using the QuickChange mutagenesis kit (Stratagene) and all mutations were confirmed by DNA sequencing (2, 3). Concentrated supernatant of lentiviral-transfected 293T cells was used to infect (i) $A2^{pos}$ and $A2^{neg}$ primary CD8 T cells ($1^{st}$ expansion), (ii) CRISPR-A2 and CRISPR-EGFP primary CD8 T cells ($2^{nd}$ expansion) or (iii) $A2^{pos}$ and $A2^{neg}$ J76 CD8αβ T cells. Primary CD8 T cells were infected overnight in plate coated with 10 $\mu g/cm^2$ retronectin (Takara), while J76 CD8αβ cells were infected for 30 min at 37°C. The transduction efficiency was 5-30% for freshly isolated CD8 T cells, 1% for $2^{nd}$ round of stimulated CRISPR-CD8 T cells, and over 96% for J76 CD8αβ cells. Integrated TCR lentiviral copy number was quantified by qPCR and was similar across TCR variants (1-2 copies/genome in primary sorted CD8 T cells and 9-26 copies/genome in J76 CD8αβ T cells) (data not shown; Supp. Table 1).

**Granzyme B and perforin staining by flow cytometry**

For intracellular staining, $3x10^5$ TCR-transduced $A2^{pos}$ and $A2^{neg}$ primary CD8 T cells from healthy individuals were fixed in PBS 1% formaldehyde, 2% glucose, and 5 mM $NaN_3$ for 20 min at room temperature, before being stained with corresponding antibodies (granzyme B and perforin) in PBS 0.2% BSA, 5 mM EDTA, 0.2% $NaN_3$, and 0.1% saponin. All experiments were performed under unstimulated, resting culture conditions. Samples were acquired with a

Gallios (Beckman Coulter) flow cytometer and data were analyzed by FlowJo software (Tree star, v10.0.8).

**CD107a degranulation assay**

$A2^{pos}$/TAP-deficient T2 cells were pulsed with 0.1 µM native NY-ESO-$1_{157-165}$ peptide for 1h at 37°C, washed and incubated with TCR-transduced $A2^{pos}$ or $A2^{neg}$ primary CD8 T cells at an effector-to-target (E:T) of 2:1 for 4h in the presence of anti-CD107a/LAMP1 and 10 µg/mL brefeldin A. Samples were acquired with a Gallios (Beckman Coulter) flow cytometer and data were analyzed by Flowjo software (Tree star).

**Chromium release assay**

The antigen recognition capacity and *in vitro* lytic activity of primary $A2^{pos}$ and $A2^{neg}$ CD8 T lymphocytes engineered with TCRs of incremental affinities were assessed using chromium release assay as previously described (4). Briefly, HLA-$A2^{pos}$/TAP-deficient T2 cells or HLA-$A2^{pos}$/NY-ESO-$1^{pos}$ Me275 cells were labeled with $^{51}Cr$. In peptide titration assay, T2 cells were pulsed with serial dilution of native NY-ESO-$1_{157-165}$ peptide and incubated for 4 h with $A2^{pos}$ or $A2^{neg}$ CD8 effector T cells at E:T ratio of 10:1. In tumor killing assay, Me275 cells were pulsed or not with 1 µM of NY-ESO-$1_{157-165}$ native peptide and incubated for 4 h with $A2^{pos}$ or $A2^{neg}$ CD8 effector T cells at indicated E:T ratios. Percentage of specific lysis was calculated as 100x (experimental-spontaneous release)/(total-spontaneous release). Dose-response curve analysis and EC50 values were obtained using Prism software (GraphPad, v.7.03).

**Functional PD1 blockade with nivolumab**

One day prior to TCR transduction, primary $A2^{pos}$ (directly isolated from a healthy donor) or $A2^{pos}$ (isolated following CRISPR/GFP transduction) CD8 T cells were cultured without (control) or with 20 µg/mL PD-1 blocking antibody (nivolumab; a gift from the Department of Oncology, University Hospital Lausanne). The culture medium containing 20 µg/mL nivolumab was constantly renewed every 3-4 days.

**Supplemental Table 1. Characteristics of affinity-increased HLA-A2/NY-ESO-1-specific TCRs**

| TCR name | NY-ESO-1-specific TCR (AV23.1/BV13.1) [a] | | | | TCR-pMHC affinity&kinetics | | quantification of TCR LV copy numbers # [e] | | | |
|---|---|---|---|---|---|---|---|---|---|---|
| | CDR2α | CDR3α | CDR2β | CDR3β | $K_D$ (μM) [a] | $t_{1/2}$ (s) [d] | CD8αβ J76 cells [f] | | primary CD8 T cells [f] | |
| | 50 51 52 53 54 55 | 93 94 95 96 97 98 | 49 50 51 52 53 54 | 95 96 97 98 99 100 | | | HLA-A2$^{pos}$ | HLA-A2$^{neg}$ | HLA-A2$^{pos}$ | HLA-A2$^{neg}$ |
| V49I | IQSSQR | RPQTGG | **I**GAGIT | VGAAGE | n.a. | 10.7 | 19 | 26 | 2.3 | 2.2 |
| WT [b] | IQSSQR | RPQTGG | VGAGIT | VGAAGE | 21.4 | 53.0 | 39 | 18 | 1.4 | 1.9 |
| A97L | IQSSQR | RPQTGG | VGAGIT | VG**L**AGE | 2.69 | 102.2 | n.d. | n.d. | n.d. | n.d. |
| DMβ | IQSSQR | RPQTGG | V**AE**GIT | VGAAGE | 1.91 | 219.7 | 20 | 20 | 1.8 | 1.1 |
| TMβ | IQSSQR | RPQTGG | V**AE**GIT | VG**L**AGE | 0.91 | 453.1 | 18 | 9 | 1.2 | 1.9 |
| QMα | IQS**W**QR | RPQTGG | V**AE**GIT | VG**L**AGE | 0.14 | 479.7 | 16 | 12 | 1.4 | 1.3 |
| wtc51m [c] | IQSSQR | RPQTGG | V**AIQT**T | VGAAGE | 0.015 | 3043.0 | 20 | 14 | 1.0 | 1.2 |
| α95:LYm [c] | IQSSQR | RP**LY**GG | VGAGIT | VGAAGE | n.a. | 172.4 | n.d. | n.d. | n.d. | n.d. |
| α95:LYm/A97L | IQSSQR | RP**LY**GG | VGAGIT | VG**L**AGE | n.a. | 260.2 | n.d. | n.d. | n.d. | n.d. |

[a] Point-mutations (in red) and molecular affinity values (by SPR) of affinity-increased TCR variants as described in (3).

[b] The wild-type BC1 TCR was isolated from melanoma patient LAU155 (5) and differs from the 1G4 TCR (6) by only 4 aa residues (underlined).

[c] NY-ESO-1-specific variants containing the wtc51 (7) or α95:LY (8) mutations within the BC1 TCR background.

[d] Monomeric TCR-pMHC off-rates ($t_{1/2}$) measured by the cell surface dissociation assay at 4°C using two-color reversible NTAmers (9).

[e] Lentiviral genomic copy number quantified by qPCR of *gag* and normalized to *albumin.*

[f] Generation of TCR-transduced HLA-A2$^{pos}$ or HLA-A2$^{neg}$ CD8αβ J76 and primary CD8 T cells as described in the Material & Methods section.

92 **Supplemental Table 2. List of antibodies used in the study**

| Targets | Color | Manufacturer | Reference |
|---|---|---|---|
| panTCRαβ | PC5 | Beckman Coulter | A39500 |
| panTCRαβ | PE | Beckman Coulter | B49177 |
| Vbeta13.1 | PE | Beckman Coulter | IM2292 |
| CD3ε | PC5.5 | BioLegend | 300430 |
| CD3ε | BrV421 | BioLegend | 300434 |
| PD-1 | APC | BioLegend | 329908 |
| PD-1 | BrV421 | BioLegend | 329920 |
| TIM-3 | PC7 | eBioscience | 25-3109-42 |
| TIGIT | APC | eBioscience | 17-9500-42 |
| 2B4 | PC5.5 | BioLegend | 329514 |
| CD69 | FITC | BD Biosciences | 347823 |
| CD25 | BrV421 | BioLegend | 302629 |
| 4-1BB | PC7 | BioLegend | 309818 |
| CD28 | BrV421 | BioLegend | 302930 |
| CD8β | PE | Beckman Coulter | IM2217U |
| CD8β | FITC | Beckman Coulter | B42025 |
| CD5 | BV421 | BioLegend | 300626 |
| CD107a | FITC | BD Bioscience | 555800 |
| Annexin V | Cy5 | BD Bioscience | 559933 |
| Ki67 | FITC | BD Bioscience | 556026 |
| Granzyme B – intracellular | FITC | BioLegend | 515403 |
| Perforin – intracellular | APC | BioLegend | 308112 |
| c-CBL – intracellular | -- | Abcam | Ab32027 |
| Secondary anti-Rabbit IgG (for c-CBL) | FITC | BD Biosciences | 554020 |
| pCD3ζ (Y142) – phospho-flow | Alexa Fluor 647 | BD Biosciences | 558489 |
| pERK71/2 (T202/Y204) - phospho-flow | Alexa Fluor 647 | Cell Signaling | 4375S |

93

94 **Supplemental Table 3. List of gene sets used for GSEA**

| | | |
|---|---|---|
| SELF TOLERANT MOUSE CD8 (10) | https://www.ncbi.nlm.nih.gov/pubmed/22267581 (CLUSTER 9 and 13) | CD81, CLSPN, CDC20, KIF15, TCF19, LOC237877, LAG3, TNFRSF9, AURKA, BCAT1, TFRC, INCENP, MCM10, HMGN3, SNN, ESPL1, HIST1H3E, CHTF18, HIST1H2BN, TNFRSF9, KNTC1, GTSE1, SGOL1, ECM1, 3000004C01RIK, HIST1H3A, TFRC, KIF2C, CDCA2, FANCD2, 2410015N17RIK, CDC6, CHAF1A, CHST2, SPAG5, HIST1H2BM, CLDN10, IGF2BP3, NHEDC2, APITD1, CCDC99, LIG1, STMN1, ZRANB3, CDC45L, MARCKSL1, RGS16, PTPLA, CHST3, CENPM, HMGN3, CDC20, PTPRS, NCAPD2, NRGN, CENPM, HIST1H3C, SOX5, HIST1H3D, CKB, NRN1, HIST1H2BH, RCC1, BUB1B, HIST1H2BJ, HIST1H2AB, TPI1, MCM5, PTPRS, NMRAL1, RAD51, CDCA7, SPC25, NDRG1, KIF4, RILPL2, PIF1, CENPM, CENPA, RAD54L, HIST1H3H, 2610510J17RIK, HIST1H2BK, HIST1H2BF, E130016E03RIK, CDC7, ITM2A, FIBCD1, XCL1, SH3BP2, TOP2A, HIST1H2AF, PPIC, HIST1H2AN, CDC2A, BIRC5, HIST1H2AG, HIST2H2AB, PPIC, LITAF, E2F2, PRC1, CDCA3, H2AFX, BIRC5, HIST1H2AH, NUSAP1, PPA1, TYMS, LOC100047934, CCNB1, PSAT1, BIRC5, PBK, HIST1H2AK, MCM6, HIST1H2AD, TYMS-PS, TPI1, UHRF1, KLRB1C, ADK, RRM1, HIST1H2AO, E2F2, TNFRSF21, 2810417H13RIK, CCNB1, SCAMP1, CHN2, LMNB1, ANLN, RRM2, PKM2, KIF22, RRM2, PLK1, MAD2L1, LOC100045304, NCAPH, E2F1, HIST2H2AC, MCM6, TK1, FEN1, CLSPN, FIGNL1, D17H6S56E-5, NDRL, CDCA3, MCM2, KIF11, CDCA5, CDC20, CHAF1B, CAPG, 3000004C01RIK, MCM10, ENDOD1, CENPH, GALK1, SWAP70, LOC100047651, GFOD1 |
| DELETIONAL TOLERANCE MOUSE CD8 (11) | https://www.ncbi.nlm.nih.gov/pubmed/19204323 (TABLE 1) | TNFSF11, RGS16, NRN1, IKZF2, TBC1D4, GPM6B, ENDOD1, FCRL1, LRIG1, LRIG1, MARCKS, NR4A3, LTA, MARCKS, SYNJ2, NR4A1, HSPA4L, PTPRS, EGR2, PSCD3, YPEL2, EGR2, SKIL, NAB2, SOAT1, GALM, TOX, 4930539E08RIK, REEP3, MDH1, 4921525O09RIK, EPHX1, SSH1, CREM, PACSIN1, LPCAT1, PRMT2, CD200R1, NRIP1, DGKZ, RASA1, H3F3B, A830073O21RIK |
| LAG3+ ANERGIC MOUSE CD4 (12) | https://www.ncbi.nlm.nih.gov/pubmed/19666526 (from analysis by (13)) | 1500004A13RIK, 1700019D03RIK, 2210010C04RIK, 2310001H17RIK, 2700008G24RIK, 2900026A02RIK, 4930452B06RIK, 4930506M07RIK, 5330417C22RIK, 5430401H09RIK, 6330403K07RIK, 6720475J19RIK, 8030451A03RIK, 9630010G10RIK, ABCB10, ABHD4, ACVR1, ADCK3, ADRBK2, AGR3, AHSP, AKR1B8, ALAS2, ALCAM, ALDH1A1, ALDH1A7, ALOX5AP, ANGPTL2, ANXA3, APOE, APOL11B, APOL8, AQP1, ARL6, ART3, ASCL2, ASNS, ATCAY, ATP2B2, ATRX, AURKB, B930095G15RIK, BC013712, BCL6, BLVRB, BMP2, BMPR2, BRCA1, BZRAP1, C2CD4B, C3, C730029A08RIK, CACNA1D, CAMK2N1, CAMP, CAPN5, CAR1, CAR2, CAR5B, CASC5, CASP3, CAV2, CC2D2A, CCDC112, CCDC28B, CCDC80, CCL1, CCL3, CCL6, CCL9, CCNB1, CCNE2, CCR8, CD109, CD200, CD24A, CD300LB, CD36, CD38, CD68, CD83, CD99L2, CDC6, CDCA8, CDKN2B, CEBPA, CEL, CELA1, CELA2A, CELA3B, CENPE, CENPK, CETN4, CHI3L3, CHN1, CHST2, CHTF18, CIT, CLDN13, CLEC4A3, CLEC4G, CLEC7A, CLIP3, CLPS, CLU, CNRIP1, COBLL1, COCH, COL4A1, COL4A2, CORO2B, CPA1, CPA2, CPB1, CREB3L2, CSDA, CSF1, CSF1R, CSF2RB, CSGALNACT1, CST7, CTGF, CTRB1, CTRL, CTSB, CTSH, CTTN, CX3CR1, CXCL10, CXCR7, CXXC5, CYBB, CYFIP1, CYP1A1, D10BWG1379E, D17H6S56E-5, D430019H16RIK, D630039A03RIK, DXERTD242E, DDC, DDX3Y, DGKI, DMBT1, DMXL2, DNAHC7B, DNASE1L3, DOCK4, DOCK7, DRAM1, DSP, DUSP14, DUSP16, DUSP4, DYNLT3, E130308A19RIK, EAR2, ECE1, EDN3, EEA1, EFNB2, EGR2, EIF2S3Y, EMILIN2, EMR4, ENPP2, ENTPD1, EOMES, EPB4.2, EPDR1, ERMAP, EVI5, EXPH5, F13A1, FAM132A, FAM20A, FAM43A, FAM55B, FAM55D, FAM59A, |

| | | |
|---|---|---|
| | | FAM81A, FAM84A, FARP1, FARP2, FBN2, FGD6, FHDC1, FIGNL1, FLRT2, FMNL2, FNDC3B, FPR2, FRMD4A, FZD6, GABARAPL1, GALM, GAS2L1, GATM, GCG, GDA, GJA1, GJB2, GLT28D2, GNA14, GNAQ, GP2, GPM6B, GPR116, GPR160, GPR35, GSTM1, GSTM5, GSTT3, GUCY1A3, GYPA, H2-AA, HAVCR2, HBB-B2, HCK, HEBP1, HEMGN, HIF1A, HIP1, HIVEP3, HJURP, HMBS, HMGN3, HP, ID2, IER5L, IFITM2, IFITM3, IFT122, IGDCC4, IGF1R, IGHM, IGHV14-2, IGSF6, IKZF2, IL10, IL1R2, IL21, ISPD, ITGB5, ITGB8, JAZF1, KDELC2, KDM5D, KEL, KIF13A, KIRREL3, KLF1, KLK1, KLRB1A, LAG3, LCN2, LIFR, LIMA1, LITAF, LMO2, LPAR3, LPL, LTF, LYN, LYZ1, LYZ2, MAF, MAGI3, MALT1, MAPRE2, 41341, MARCKSL1, MATN2, MET, MFSD2B, MGST1, MMD, MMP14, MPEG1, MPO, MT1, MTAP2, MTMR7, MYH10, MYH3, MYO1E, NA, NANOS1, NCAPG, NCRNA00086, NDN, NDRG4, NF2, NFATC1, NFE2, NFIL3, NGP, NHEDC2, NPAS4, NPNT, NR4A2, NRBP2, NRN1, NRP1, NT5E, NTF5, NTRK3, NUDT6, OCLN, ORC1, PADI4, PBK, PBX3, PDCD1, PDGFRL, PDZK1IP1, PDZRN3, PENK, PERP, PEX11A, PHACTR2, PISD-PS3, PKD2, PLAGL1, PLEK, PLEKHO1, PLOD2, PLSCR4, PLXDC2, PLXNB2, PNLIP, PNLIPRP1, PNLIPRP2, PPAP2A, PRELID2, PRKAR2B, PRKCA, PRNP, PRPF40A, PRSS2, PTGER2, PTGFRN, PTPLA, PTPN11, PTPN13, PTPN5, PTPRB, PTPRJ, PTPRS, PYGL, RAB39B, RALYL, RAPGEF5, RASSF6, RBM5, RBPJ, RCAN1, REEP1, REG1, RGS16, RHAG, RHD, RNASE1, RNF128, RPS6KC1, S100A10, S100A8, S100A9, S1PR3, SAMD11, SCCPDH, SCIN, SCLY, SDPR, SDR39U1, SEC16B, SEMA4C, SEMA7A, SERPINA9, SERPINC1, SERPINF1, SH3GL3, SH3RF1, SIRPB1A, SLC1A4, SLC22A15, SLC24A3, SLC25A13, SLC29A1, SLC35F5, SLC37A2, SLC38A5, SLC4A1, SLC5A3, SLC6A8, SLC7A10, SMC2, SMPDL3B, SNCA, SOSTDC1, SOX6, SPAG5, SPARC, SPIN4, SPIRE1, SPNA1, SPOCK2, SPP1, SRGAP3, SRXN1, STAB2, STC2, STFA3, STOM, STX11, SUSD2, SYNPO, SYT11, TAL1, TBC1D4, TCEAL8, TEX15, TFPI, TFRC, TG, TGFBI, TGM2, TIAM2, TIMP2, TJP1, TJP2, TM4SF1, TMBIM1, TMCC2, TMCC3, TMEM2, TMEM26, TMEM56, TMPRSS11E, TNFAIP2, TNFAIP8, TNFRSF9, TNFSF8, TNFSF9, TOX, TPMT, TREML4, TRFR2, TRIM10, TRIM12A, TRPS1, TSC1, TSHZ2, TSPAN2, TSPAN33, TSPAN8, TWSG1, UBR2, UHRF1, UNC13B, UTY, VAT1L, VDR, VSIG10, WIPF3, WISP1, ZBTB32, ZEB2, ZER1, ZFP612, ZG16 |

95

## SUPPLEMENTAL FIGURE LEGENDS

**Supplemental Figure 1. Characterization and baseline expression of TCR/CD3 complex in *de novo* HLA-A2-expressing Jurkat J76 CD8αβ T cells. (A)** Representative histograms of surface markers on the parental Jurkat J76 CD8αβ cell line. Gray histograms correspond to unstained cells and colored histograms to cells stained with the indicated antibodies. **(B)** Representative histograms of HLA-A2 and HLA-A3 expression on codon-optimized A2-transduced J76 CD8αβ cells ($A2^{pos}/A3^{pos}$), parental J76 CD8αβ cells ($A2^{neg}/A3^{pos}$), T2 cells ($A2^{pos}/A3^{neg}$), and C1R cells ($A2^{neg}/A3^{pos}$). **(C)** Killing assays with NY-ESO-1-specific $A2^{neg}$ CD8 T cells (DMβ TCR variant) as effectors and indicated cells as targets, in the presence of increased concentrations of NY-ESO-$1_{157-165}$ native peptide. **(D)** Representative histograms of expression levels of the TCR/CD3 complex (panTCRαβ, Vβ13.1 and CD3ε) under steady-state culture conditions, in absence of antigen-specific stimulation. **(E)** Quantification of the expression of surface (i.e. extracellular) CD3ε and of total (i.e. intra- and extracellular) CD3ε. **(C and E)** Data are representative of 2 to 3 independent experiments.

**Supplemental Figure 2. Phosphorylation levels of CD3ζ and ERK upon stimulation and basal expression levels of surface receptors in $A2^{pos}$ and $A2^{neg}$ J76 CD8αβ T cells. (A)** Representative histograms of phosphorylation levels of CD3ζ and ERK1/2 after stimulation (with NY-ESO-1 multimer, OKT-3 or PMA/ionomycin) in $A2^{pos}$ (red histograms) and $A2^{neg}$ (blue histograms) J76 CD8αβ cells. **(B, C)** Representative histograms of CD5 and c-CBL expression **(B)** and of PD-1 and CD69 expression **(C)** in $A2^{pos}$ (red histograms) versus $A2^{neg}$ (blue histograms) J76 CD8αβ cells, under resting conditions.

**Supplemental Figure 3. Basal expression levels of co-activating/inhibitory receptors on $A2^{pos}$ and $A2^{neg}$ primary CD8 T cells upon affinity-increased TCR transduction. (A)** Representative histograms of the expression levels of co-activating/inhibitory receptors on $A2^{pos}$ (CRISPR/GFP) and $A2^{neg}$ (CRISPR/A2) primary CD8 T cells post-TCR transduction, in the absence of cognate antigen. Of note, no difference in any surface marker was observed between $A2^{pos}$ and $A2^{neg}$ untransduced CD8 T cells (gray histograms). **(B)** Relative expansion of $A2^{pos}$ (red lines) versus $A2^{neg}$ (blue lines) tumor-specific CD8 T cells upon TCR transduction, represented as NY-ESO-$1^{pos}$ T cell fraction (upper panels) or as NY-ESO-$1^{pos}$ variations from the initial transduction efficiency (bottom panels). Data are representative of 5 to 10 experiments.

**Supplemental Figure 4. Surface staining and population doublings of primary A2$^{pos}$ CD8 T cells with or without PD-1 blocking antibody. (A)** Representative histograms of expression levels of co-activating/inhibitory receptors in A2$^{pos}$ (CRISPR/A2) CD8 T cells post-TCR transduction, cultured over time with or without 20 µg/mL of nivolumab. **(B)** Population doublings of TCR-transduced A2$^{pos}$ (CRISPR/A2) CD8 T cells cultured in the presence or the absence of 20 µg/mL nivolumab were assessed by periodic cell counting of living cells during 10 days and in the absence of cognate antigen. Data are representative of two independent experiments.

**Supplemental Figure 5. Gene Set Enrichment Analysis (GSEA) of high-affinity versus optimal TCR variants.** Genome-wide microarray analysis was previously performed on A2$^{pos}$ primary CD8 T cells engineered with our panel of TCR variants against NY-ESO-1 (GSE42922) (2). **(A, B)** GSEA of available gene sets describing anergy (12), self-tolerance (10), and deletional tolerance (11) were found enriched in A2$^{pos}$ CD8 T cells expressing **(A)** the high-affinity TCR wtc51m variant versus the wild-type one and **(B)** the high-affinity (i.e. TMα and wtc51m) relative to optimal-affinity TCR variants (i.e. G50A and DMβ), under steady-state culture conditions. Nominal p values and false discovery rates (FDR) are indicated for each gene set enrichment.

**Supplemental Figure 6. CD107a degranulation and killing capacity of A2$^{pos}$ and A2$^{neg}$ primary CD8 T cells expressing affinity-increased TCRs. (A)** Baseline expression levels of granzyme B and perforin in A2$^{pos}$ and A2$^{neg}$ primary CD8 T cells. **(B)** CD107a degranulation of A2$^{pos}$ and A2$^{neg}$ primary CD8 T cells upon stimulation with native NY-ESO-1 peptide-pulsed T2 cells at 0.1 µM. **(C)** Representative graphs (left panel) and quantification (right panel) of killing of Me275 cells pulsed with 1 µM of NY-ESO-1$_{157-165}$ native peptide at the indicated E:T ratios. **(D)** Representative graphs (left panel) and quantification of EC50 values (right panel) of killing of T2 cells pulsed with different concentrations of NY-ESO-1$_{157-165}$ native peptide (pp), at an E:T ratio of 10:1 by chromium release assays. **(A-D)** Data are means ± SD of 4-6 independent experiments.

**Supplemental Figure 7**. **Expression levels of PD-1 and CD69 in A2$^{neg}$ J76 CD8αβ cells during 14 days of co-culture with NA8 tumor cells. (A)** Schematic representation of the experimental design; A2$^{neg}$ J76 CD8αβ T cells of increased-affinity TCRs were co-cultured with either A2$^{pos}$ or A2$^{neg}$ NA8 tumor cells for 14 days in the absence of cognate antigen. **(B)**

Expression levels of PD-1 and CD69 on $A2^{neg}$ J76 CD8αβ cells were performed at day 2, 4, 7, 10 and 14 of co-culture with either $A2^{pos}$ or $A2^{neg}$ NA8 tumor cells. Data are means ± SD of two independent co-culture experiments (n = 10). Matched P values are by two-way ANOVA followed by Sidak's multiple comparisons test; * $P \leq 0.05$ and **** $P \leq 0.0001$.

**Supplemental Figure 8**. **Dynamics of $A2^{pos}$ versus $A2^{neg}$ redirected primary CD8 T cell sub-populations in co-cultures following TCR transduction. (A)** Schematic representation of the $A2^{pos}$ (CRISPR/mock) and $A2^{neg}$ (CRISPR/A2) CD8 T cell co-cultures at an initial ratio of 1:1. TCR-untransduced CD8 T cells are depicted as gray-filled circles. **(B)** Flow cytometry gating (left panels) and quantification of $A2^{pos}$ and $A2^{neg}$ sub-populations (right panels) at the indicated days following TCR transduction and according to the different TCR affinity variants.

## REFERENCES


1. Ran FA, Hsu PD, Wright J, Agarwala V, Scott DA, and Zhang F. Genome engineering using the CRISPR-Cas9 system. *Nat Protoc.* 2013;8(11):2281-308.
2. Hebeisen M, Baitsch L, Presotto D, Baumgaertner P, Romero P, Michielin O, et al. SHP-1 phosphatase activity counteracts increased T cell receptor affinity. *J Clin Invest.* 2013;123(3):1044-56.
3. Irving M, Zoete V, Hebeisen M, Schmid D, Baumgartner P, Guillaume P, et al. Interplay between T cell receptor binding kinetics and the level of cognate peptide presented by major histocompatibility complexes governs CD8+ T cell responsiveness. *J Biol Chem.* 2012;287(27):23068-78.
4. Allard M, Couturaud B, Carretero-Iglesia L, Duong MN, Schmidt J, Monnot GC, et al. TCR-ligand dissociation rate is a robust and stable biomarker of CD8+ T cell potency. *JCI Insight.* 2017;2(14).
5. Derre L, Bruyninx M, Baumgaertner P, Ferber M, Schmid D, Leimgruber A, et al. Distinct sets of alphabeta TCRs confer similar recognition of tumor antigen NY-ESO-1157-165 by interacting with its central Met/Trp residues. *Proc Natl Acad Sci U S A.* 2008;105(39):15010-5.
6. Chen JL, Stewart-Jones G, Bossi G, Lissin NM, Wooldridge L, Choi EM, et al. Structural and kinetic basis for heightened immunogenicity of T cell vaccines. *J Exp Med.* 2005;201(8):1243-55.
7. Dunn SM, Rizkallah PJ, Baston E, Mahon T, Cameron B, Moysey R, et al. Directed evolution of human T cell receptor CDR2 residues by phage display dramatically enhances affinity for cognate peptide-MHC without increasing apparent cross-reactivity. *Protein Sci.* 2006;15(4):710-21.
8. Robbins PF, Li YF, El-Gamil M, Zhao Y, Wargo JA, Zheng Z, et al. Single and dual amino acid substitutions in TCR CDRs can enhance antigen-specific T cell functions. *J Immunol.* 2008;180(9):6116-31.
9. Hebeisen M, Schmidt J, Guillaume P, Baumgaertner P, Speiser DE, Luescher I, et al. Identification of Rare High-Avidity, Tumor-Reactive CD8+ T Cells by Monomeric TCR-Ligand Off-Rates Measurements on Living Cells. *Cancer Res.* 2015;75(10):1983-91.
10. Schietinger A, Delrow JJ, Basom RS, Blattman JN, and Greenberg PD. Rescued tolerant CD8 T cells are preprogrammed to reestablish the tolerant state. *Science.* 2012;335(6069):723-7.
11. Parish IA, Rao S, Smyth GK, Juelich T, Denyer GS, Davey GM, et al. The molecular signature of CD8+ T cells undergoing deletional tolerance. *Blood.* 2009;113(19):4575-85.
12. Okamura T, Fujio K, Shibuya M, Sumitomo S, Shoda H, Sakaguchi S, et al. CD4+CD25-LAG3+ regulatory T cells controlled by the transcription factor Egr-2. *Proc Natl Acad Sci U S A.* 2009;106(33):13974-9.
13. Martinez GJ, Pereira RM, Aijo T, Kim EY, Marangoni F, Pipkin ME, et al. The transcription factor NFAT promotes exhaustion of activated CD8(+) T cells. *Immunity.* 2015;42(2):265-78.

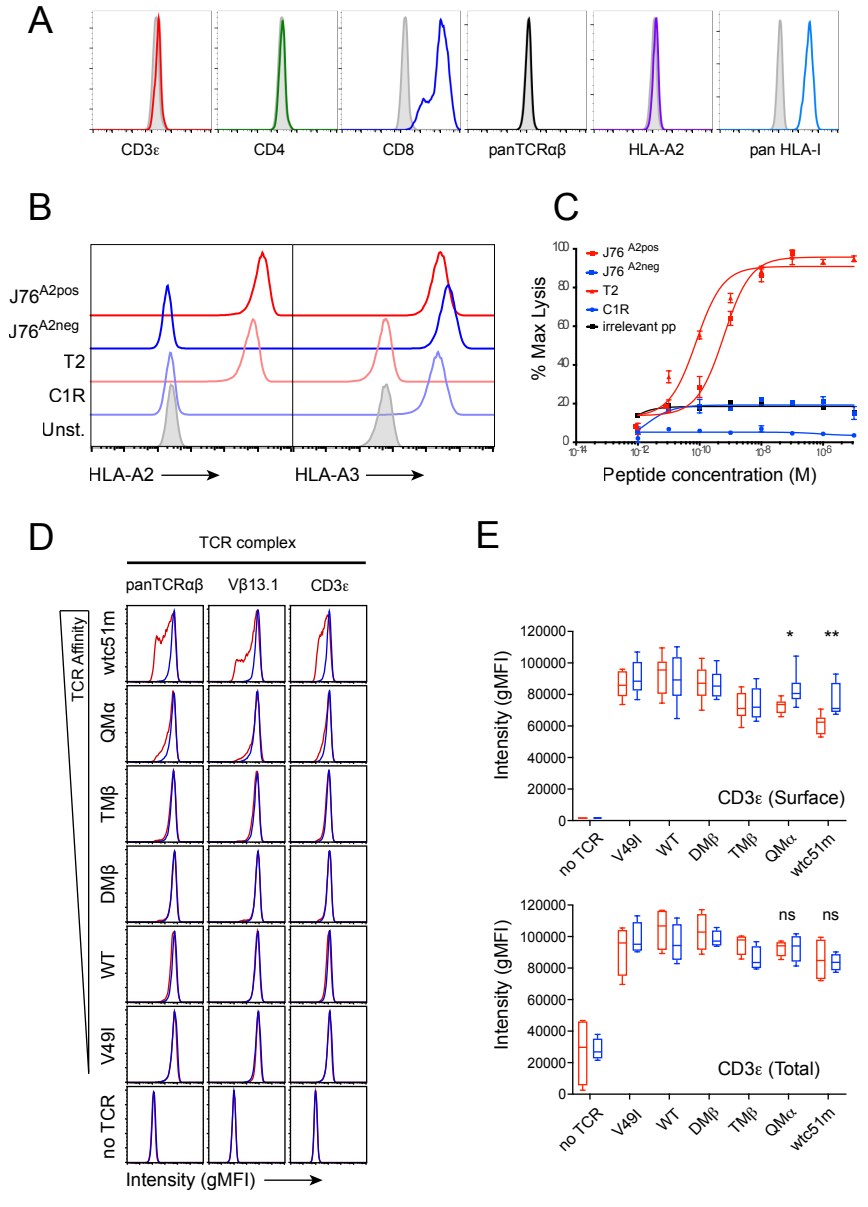


Supplementary FIGURE 1 - Duong et al.

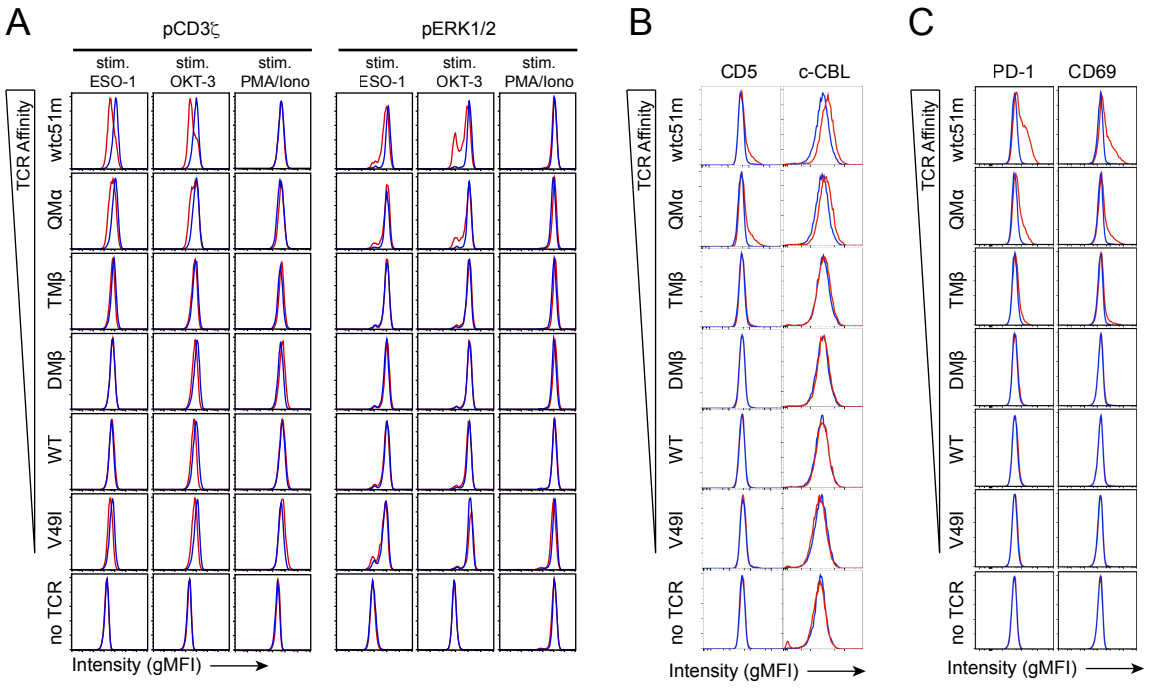


Supplementary FIGURE 2 - Duong et al.

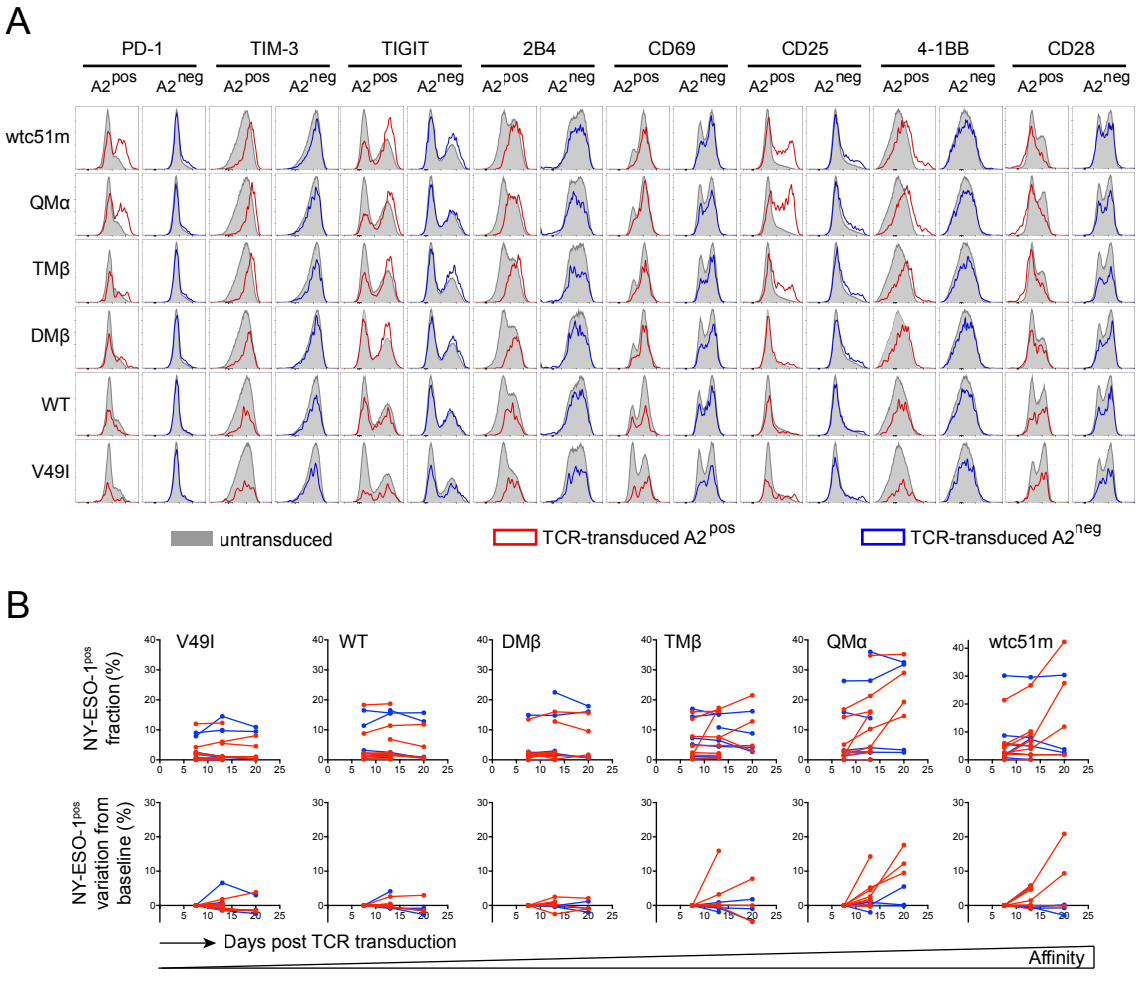


Supplementary FIGURE 3 - Duong et al.

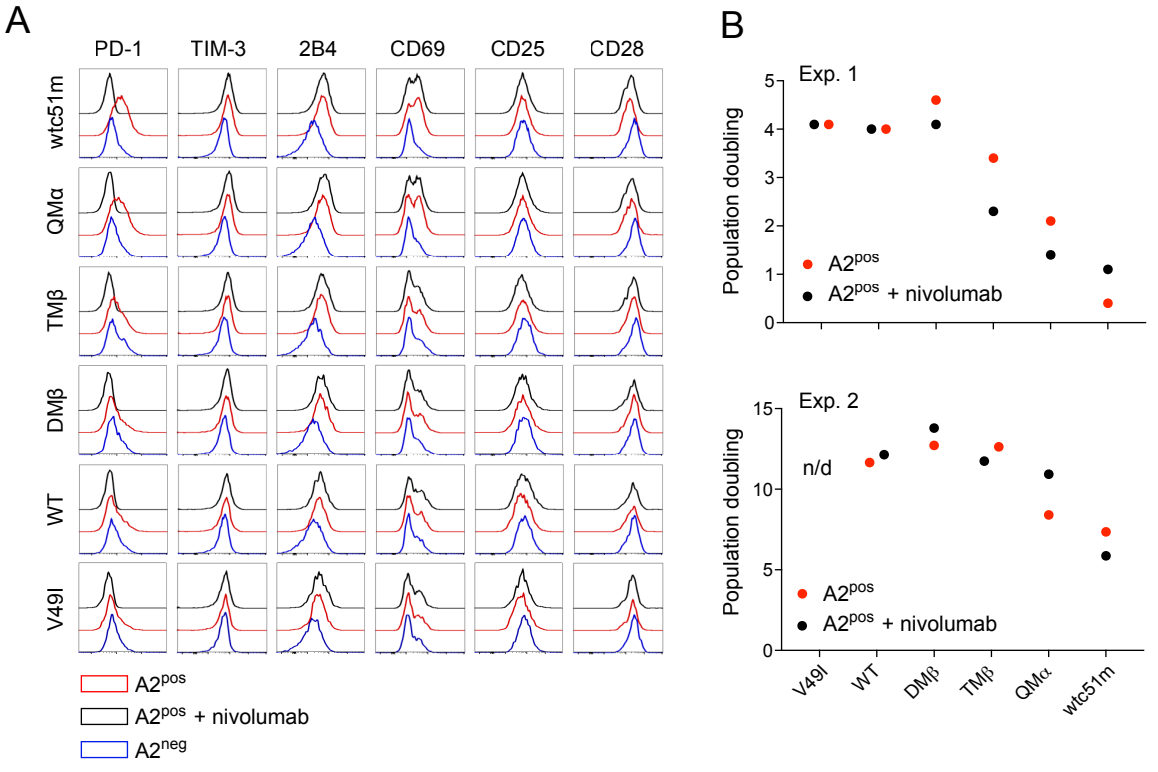


Supplementary FIGURE 4 - Duong et al.

**Gene set enrichment analyses (GSEA) at baseline**

A wtc51m vs. wild-type

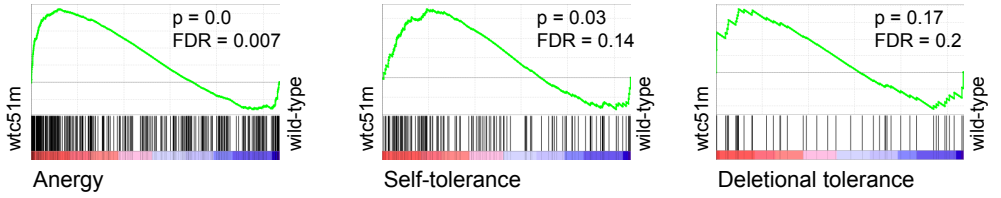


B high vs. optimal TCR affinity variants

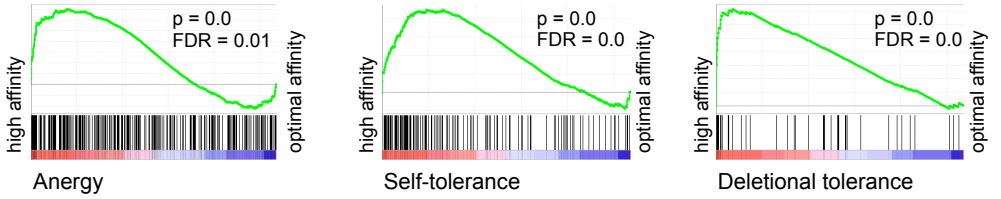


Supplementary FIGURE 5 - Duong et al.

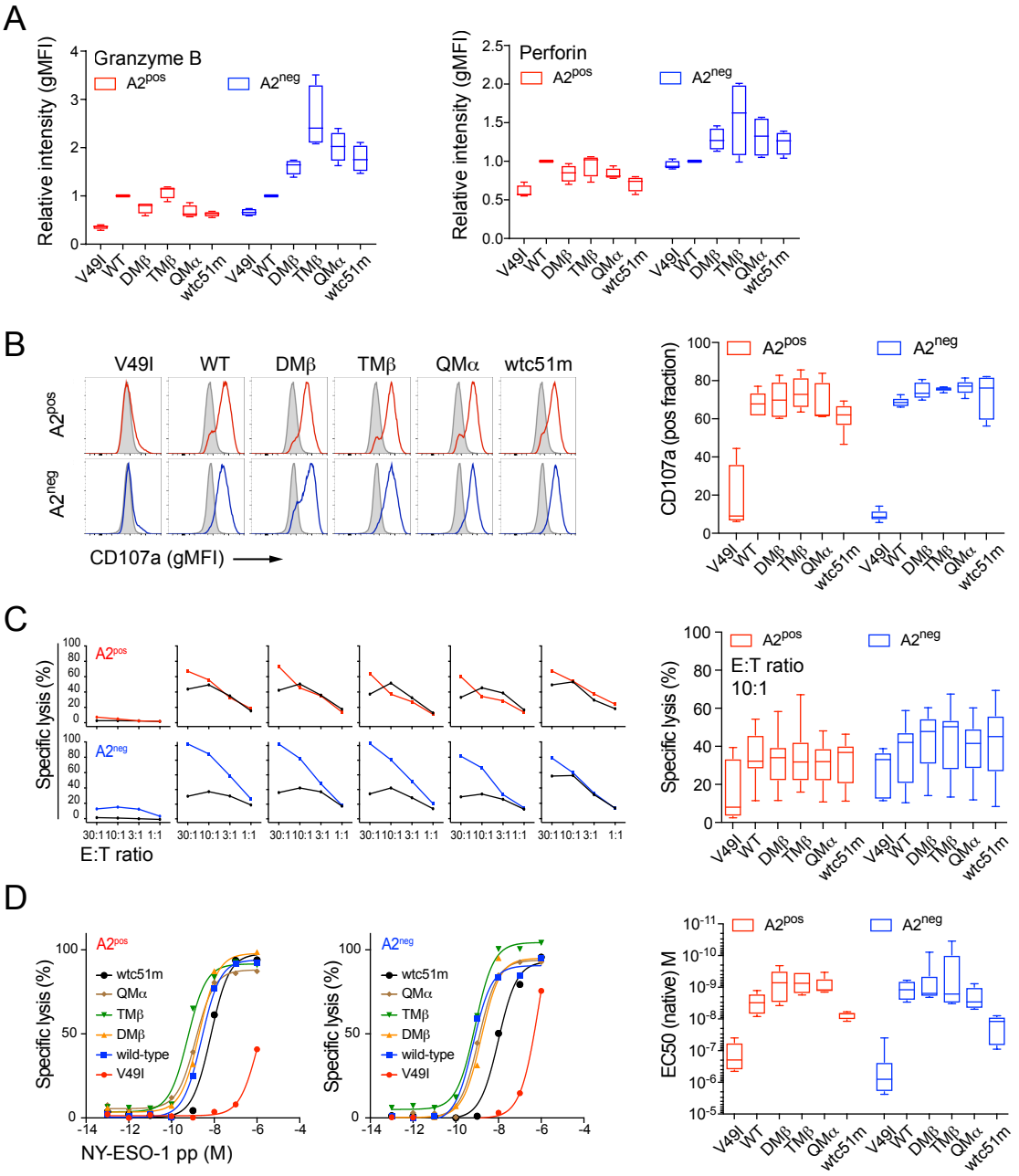


Supplementary FIGURE 6 - Duong et al.

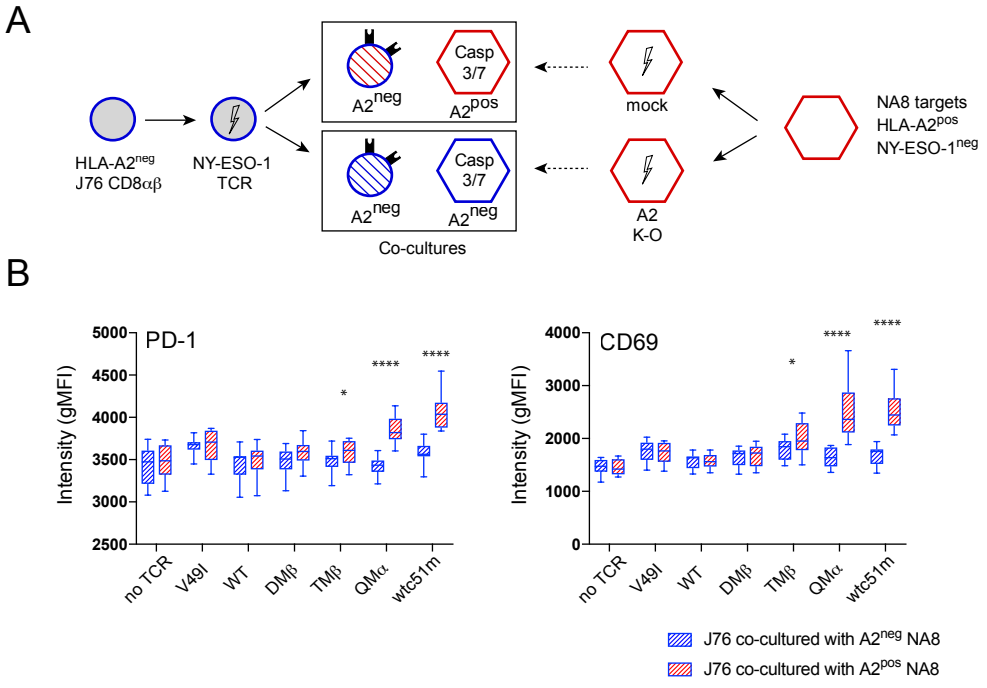


Supplementary FIGURE 7 - Duong et al.

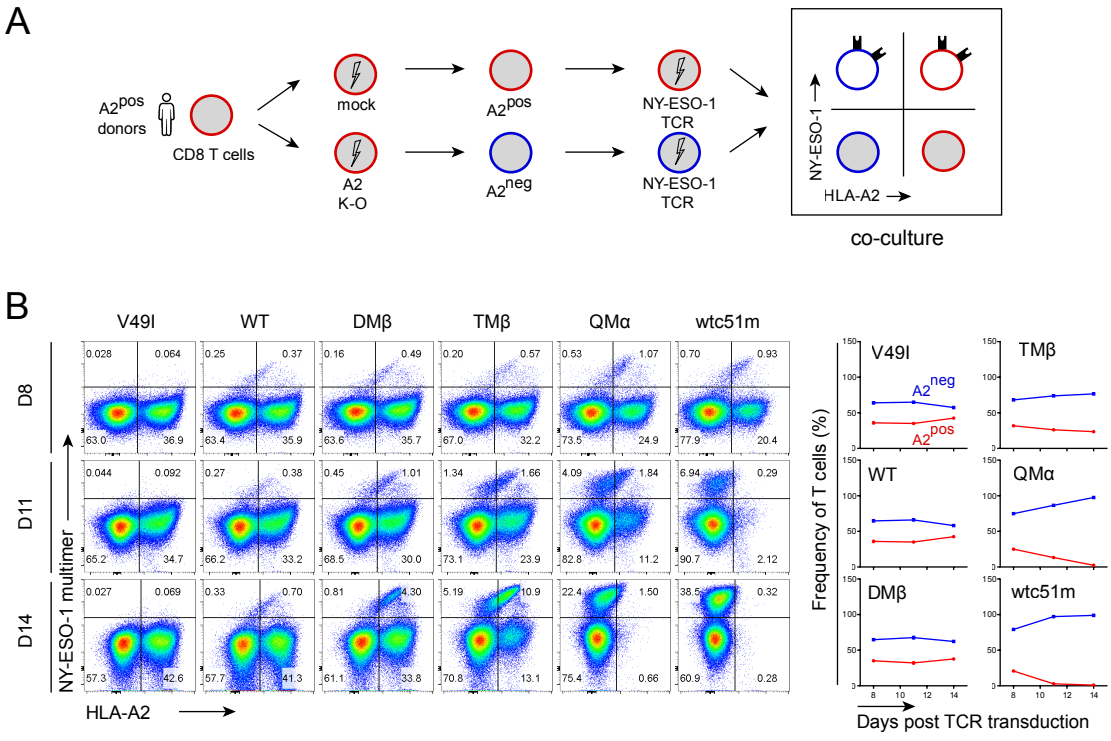


Supplementary FIGURE 8 - Duong et al.